

Coulomb-Enhanced Spin-Orbit Splitting: The Missing Piece in the Sr₂RhO₄ Puzzle

Guo-Qiang Liu, V. N. Antonov, O. Jepsen, and O.K. Andersen.
Max-Planck Institut für Festkörperforschung, D-70569 Stuttgart, Germany
(Dated: November 8, 2018)

The outstanding discrepancy between the measured and calculated (local-density approximation) Fermi surfaces in the well-characterized, paramagnetic Fermi liquid Sr₂RhO₄ is resolved by including the spin-orbit coupling and Coulomb repulsion. This results in an effective spin-orbit coupling constant enhanced 2.15 times over the bare value. A simple formalism allows discussion of other systems. For Sr₂RhO₄, the experimental specific-heat and mass enhancements are found to be 2.2.

PACS numbers: 71.18.+y, 71.20.-b, 71.30.+h

Since the discoveries of high-temperature superconductivity and colossal magnetoresistance in Mott insulators made metallic by hole-doping, transition-metal oxides have remained at the forefront of research. Their many lattice and electronic (orbital, charge, and spin) degrees of freedom are coupled by effective interactions (electron-phonon, hopping, t , Coulomb repulsion, U , and Hund's-rule coupling, J), and when some of these are of similar magnitude, competing phases may exist in the region of controllable compositions, fields, and temperatures. The interactions tend to remove low-energy degrees of freedom, e.g. to reduce the metallicity. This rarely happens by merely shifting spectral weight from a quasiparticle band into incoherent Hubbard bands, as in the U/t -driven metal-insulator transition for the single-band Hubbard model, but is usually assisted by lattice distortions which break the degeneracy of low-energy orbitals and split the corresponding quasiparticle –or partly incoherent– bands away from the chemical potential. According to recent calculations using the local density-functional plus *dynamical* mean-field approximation (LDA+DMFT), such Coulomb-enhanced crystal-field splitting seems to be the mechanism triggering the expansion-induced metal-insulator transition in undoped LaMnO₃ [1] and in V₂O₃ [2], long considered the prototype Mott transition. The low-temperature, antiferromagnetically-ordered, insulating phase of V₂O₃ is well described [3] in the LDA+ U *static* mean-field approximation, which yields the configuration $t_{2g}^2 \rightarrow e_g^{\pi \uparrow \uparrow} a_{1g}^0$. Although this approximation exaggerates the tendency towards symmetry breaking, it does give a reasonable description of the shape of the Fermi surface (FS) on the metallic side of the transition [1, 2].

When going from $3d$ to $4d$ transition-metal oxides, the larger extent of the $4d$ orbitals cause the hopping, t , and the coupling to the lattice to increase, and U and J to decrease. This is reflected in the rich electronic properties of e.g. the t_{2g}^4 ruthenates in the Ruddlesden-Popper series (Ca_{1-x}Sr_x) _{ν +1}Ru _{ν} O_{3 ν +1} [4, 5, 6, 7, 8]. Here, the end-members ($\nu=1$ and $\nu=\infty$) have the same structures as respectively La₂CuO₄ (2D K₂NiF₄-type) and LaMnO₃ (3D perovskite). The relatively small size and strong covalency of the Ca ions cause the RuO₆ octahedra to

rotate and tilt. The resulting misalignment of the Ru t_{2g} Wannier orbitals (WOs) reduces the hopping between them, and so does the deformation of the WO's caused by Ca-O- t_{2g} covalency [9, 10]. As a result, the 2D materials with $x \lesssim 0.1$ are Mott-insulators. Ca₂RuO₄ is insulating below 360 K, has orbital order with flat octahedra below 260 K [11], and is antiferromagnetic below 110 K with configuration $xy^{\uparrow \downarrow} xz^{\uparrow} yz^{\uparrow}$ according to the LDA+ U [12, 13]. Moderate pressure induces a first order transition to a metallic state with reduced tilt and rotation, and with ferromagnetic order at low temperature [14, 15, 16]. For $x \gtrsim 0.1$ the materials are metallic and exhibit metamagnetism coupled to structural distortions as long as $x \leq 0.25$ [17, 18]. The properties of the ruthenates with $x \gtrsim 0.1$ seem to be well described [13, 19, 20, 21, 22, 23, 24] in the spin-unrestricted LDA (LSDA), a parameter-free approximation which essentially neglects U , and substitutes J by the Stoner exchange coupling. For Ca_{1.5}Sr_{0.5}RuO₄ at 40 K, angle-resolved photoemission spectroscopy (ARPES) gives a FS which –after paying due attention to surface reconstruction– is found [25] to have neither orbital nor spin-polarization, and to be in good agreement with the LDA. Finally, stoichiometric Sr₂RuO₄ is tetragonal and becomes superconducting below 1 K, presumably with spin-triplet p -wave pairing [26, 27]. Both dHvA [28] and ARPES [29, 30] measurements show that, at low temperature, Sr₂RuO₄ is a nearly 2D Fermi liquid whose FS agrees well with the LDA [19, 20] and a mass-enhancement of about 3.

In view of this decreasing strength of the Coulomb correlations, it therefore came as a surprise when dHvA and ARPES [31, 32, 33] at ~ 10 K showed Sr₂RhO₄, also a paramagnetic Fermi liquid with similar structure and electron-electron interactions but one more electron, to have a FS in substantial disagreement with the LDA. The initial surprise was that the experimental FS has no xy sheet, but it was soon realized [31, 34] that in the K₂NiF₄ structure the 2D xy and $x^2 - y^2$ bands are so broad that they overlap at the d^5 Fermi level, and that the observed [35] relaxation by alternating rotations of the neighboring, corner-sharing RhO₆ octahedra around their z -axes, is such as to *gap* those two bands. As a consequence, only the equivalent 1D xz and yz bands,

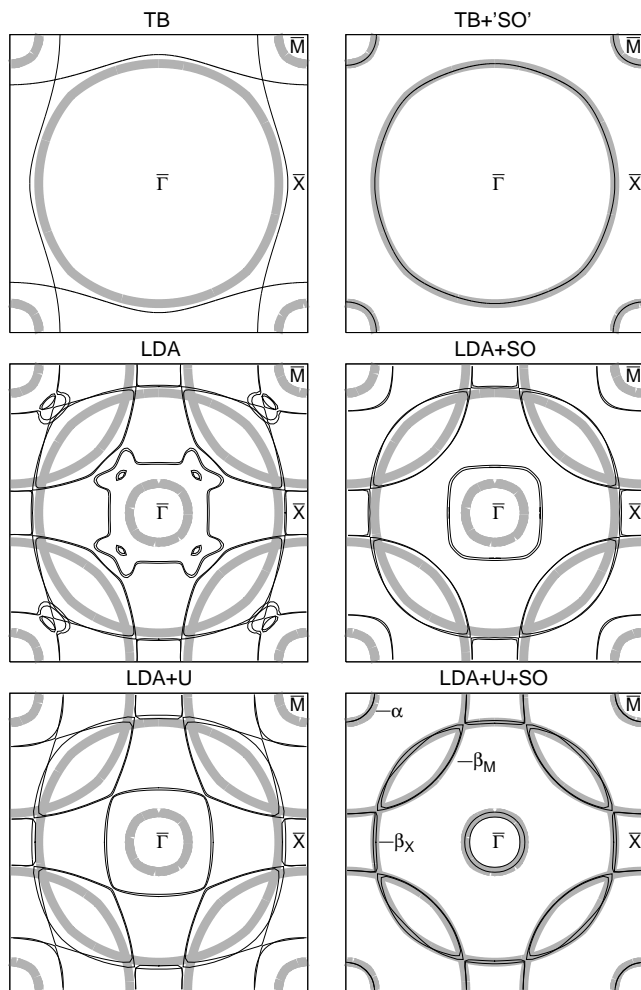


FIG. 1: FS of Sr_2RhO_4 in the $k_z=0$ plane of the large Brillouin zone centered at $(k_x, k_y) = (0, 0) \equiv \bar{\Gamma}$, with corners at $(\pi, \pi) \equiv \bar{M}$, and edge-midpoints at $(\pi, 0) \equiv \bar{X}$, in units of the inverse Rh-Rh nearest-neighbor distance. *Grey*: ARPES [31, 33], the same FS in all six pictures, but unfolded in the top panels. *Black*: Theory using six different approximations. The top panels results from the analytical expressions and parameter values given in the text and employs one xz and one yz orbital per cell. The remaining pictures result from all-orbital LDA[36] calculations for the proper crystal structure with 4 formula units per cell [35]. The conventional Fermi-sheet notation is given in the (LDA+U+SO) picture.

which hardly hybridize with the other d bands nor with each other, remain at the Fermi level with the single t_{2g} hole distributed equally between them. However, also the LDA FS calculated for the proper structure deviates substantially from the experimental FS [31, 32, 33]. This discrepancy clearly seen in Fig. 1 (LDA) is disturbing because there is no experimental indication of any further distortion. Hence, Coulomb-enhanced crystal-field splitting can not be the solution to this puzzle.

In this Letter we shall argue that the clue is *Coulomb-enhanced spin-orbit (SO) splitting*. We begin by demon-

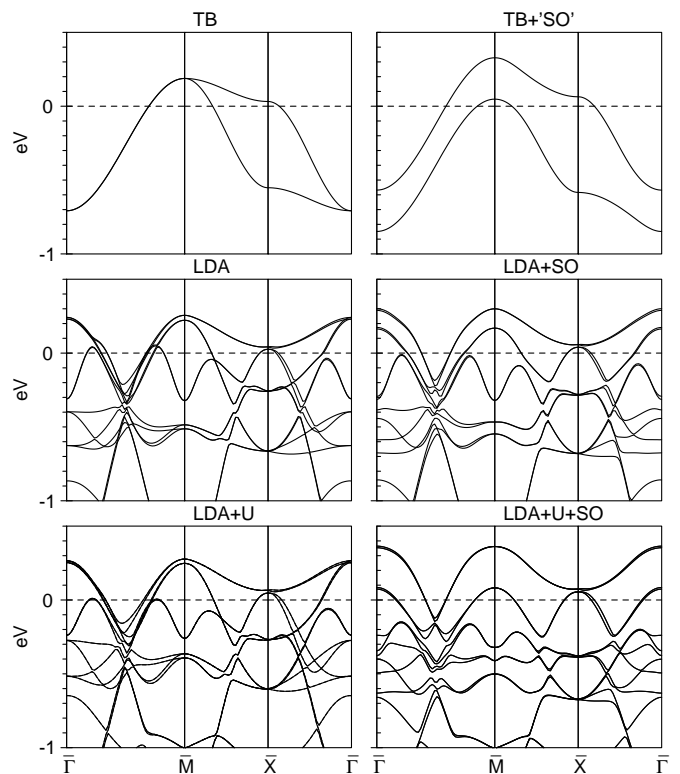


FIG. 2: Theoretical band structure of Sr_2RhO_4 in the six different approximations. See Fig. 1.

strating that the experimental FS can be perfectly fitted and the low-energy band structure explained using simple, analytical theory. These results are illustrated in the top panels of Figs. 1 and 2. We then perform *ab initio* LDA calculations [36] including the SO coupling (LDA+SO), and later also on-site Coulomb effects in the LDA+U approximation. The detailed results in the 2nd and 3rd panels of Figs. 1 and 2 prove the soundness of our simple theory.

In the Hilbert space of only the xz and yz WOs, the 2D translational symmetry is a quadratic lattice with *one* Rh per cell; the relative rotation of the nearest-neighbor RhO_6 octahedra merely modifies the hopping integrals [9]. In the z -direction the hopping is small and not detected in ARPES. Neglecting it, as well as the small rotation-induced hopping between the xz and yz bands, the electron dispersion is [9, 38]:

$$\varepsilon_{xz}^{\mathbf{k}} = -2t_{\pi} \cos k_x - 2t_{\delta} \cos k_y - \varepsilon_F, \quad (1)$$

and equivalently for $\varepsilon_{yz}^{\mathbf{k}}$. Here, ε_F is the position of the Fermi level with respect to the energy at $\bar{\Gamma}\bar{M}/2$ and signs have been chosen such that the hopping integrals are positive: $t_{\pi} \sim t_{pd\pi}^2 / (\varepsilon_F - \varepsilon_p)$ because this hop is mainly via the $O p_z$ orbital, and $0 < t_{\delta} \ll t_{\pi}$ because this hop is direct $dd\delta$. These tight-binding bands are shown in Fig. 2(TB). In the space of the $(xz \uparrow, xz \downarrow, yz \uparrow, yz \downarrow)$

WOs, the eigenfunctions of the SO coupling are:

$$\chi_{m_j=\frac{3}{2}} = (xz + iy z) \uparrow \text{ and } \chi_{-\frac{3}{2}} = (xz - iy z) \downarrow$$

with eigenvalue $\frac{1}{2}\zeta$ (> 0), and

$$\chi_{\frac{1}{2}} = (xz + iy z) \downarrow \text{ and } \chi_{-\frac{1}{2}} = (xz - iy z) \uparrow$$

with eigenvalue $-\frac{1}{2}\zeta$. SO coupling thus splits the degeneracy of the xz and yz bands along $\bar{\Gamma}\bar{M}$ by ζ as seen in Fig. 2 (TB+'SO'). Since the structure has inversion symmetry, all bands remain doubly degenerate. The band structure is given by:

$$\varepsilon_{\pm}^{\mathbf{k}} = \frac{1}{2} \left[\varepsilon_{xz}^{\mathbf{k}} + \varepsilon_{yz}^{\mathbf{k}} \pm \sqrt{(\varepsilon_{xz}^{\mathbf{k}} - \varepsilon_{yz}^{\mathbf{k}})^2 + \zeta^2} \right], \quad (2)$$

and the FS, $\varepsilon_{\pm}^{\mathbf{k}}=0$, is determined by merely 3 parameters, t_{π}/ε_F , t_{δ}/ε_F , and ζ/ε_F , which may be obtained by fitting to 3 FS dimensions, e.g. the two intersections along $\bar{\Gamma}\bar{M}$ and the one along $\bar{\Gamma}\bar{X}$. Fitting in this way to the ARPES FS [33], *perfect agreement* with the *entire* FS is obtained as seen in Fig. 1 (TB+'SO'). The area of the $\bar{\Gamma}$ -centered electron sheet *minus* that of the \bar{M} -centered hole sheet equals half the Brillouin-zone area. As seen in Fig. 1 (LDA+SO), the agreement with ARPES is less good for the ab initio relativistic LDA FS: the SO splitting along $\bar{\Gamma}\bar{M}$ is too small. In fact, fitting the LDA+SO FS to our analytical expression, yields essentially the same values for t_{π}/ε_F and t_{δ}/ε_F , but ζ/ε_F is smaller than $\zeta_{\text{ARPES}}/\varepsilon_F$ by the *large factor* 2.15. The LDA+SO calculation (Fig. 2) yields: $\zeta = 0.13$ eV, a value which is smaller than the 0.16 eV obtained for elemental fcc Rh [39] due to the $O p_z$ tails of the rhodate WOs. Letting ζ set the energy scale of bare bands, the TB+'SO' parameters reproducing the ARPES FS are: $\zeta_{\text{ARPES}} = 2.15 \times 0.13$ eV = 0.28 eV, $\varepsilon_F = 0.260$ eV, $t_{\pi} = 0.185$ eV and $t_{\delta} = 0.039$ eV. The TB results in Figs 1 and 2 are obtained with $\zeta = 0$.

In order to explain the origin of the SO-*enhancement*, we need to add the on-site Coulomb repulsion, $\hat{H}_{\text{SO}}^{\mathbf{n}}$, and thus consider the 2-band Hubbard Hamiltonian:

$$\hat{H} = \sum_{\mathbf{k}} \sum_{\mu=xz,yz} \sum_{\sigma} \varepsilon_{\mu}^{\mathbf{k}} \hat{c}_{\mu\sigma}^{\mathbf{k}} \dagger \hat{c}_{\mu\sigma}^{\mathbf{k}} + \sum_{\mathbf{n}} \left(\hat{H}_{\text{SO}}^{\mathbf{n}} + \hat{H}_{\text{C}}^{\mathbf{n}} \right), \quad (3)$$

$\varepsilon_{\mu}^{\mathbf{k}}$ given by Eq.(1) and $\mathbf{n} \equiv (n_x, n_y)$ runs over the quadratic lattice. For simplicity, we drop the superscripts \mathbf{n} in the following. The SO interaction is:

$$\hat{H}_{\text{SO}} = \frac{\zeta}{2} \left(\hat{n}_{\frac{3}{2}} + \hat{n}_{-\frac{3}{2}} - \hat{n}_{\frac{1}{2}} - \hat{n}_{-\frac{1}{2}} \right) \equiv -\frac{\zeta}{2} \hat{p}, \quad (4)$$

where \hat{n}_{m_j} is an electron-number operator and \hat{p} is the difference between $|m_j|=\frac{3}{2}$ and $|m_j|=\frac{1}{2}$, i.e.: the SO polarization. The Coulomb repulsion is U between two electrons with the same orbital, $U-2J$ between electrons with

different orbitals and different spins, and $U-3J$ between electrons with different orbitals:

$$\begin{aligned} \hat{H}_{\text{C}} = & U \left(\hat{n}_{\frac{3}{2}} \hat{n}_{\frac{1}{2}} + \hat{n}_{-\frac{3}{2}} \hat{n}_{-\frac{1}{2}} \right) \\ & + (U - 2J) \left(\hat{n}_{\frac{3}{2}} \hat{n}_{-\frac{3}{2}} + \hat{n}_{\frac{1}{2}} \hat{n}_{-\frac{1}{2}} \right) \\ & + (U - 3J) \left(\hat{n}_{\frac{3}{2}} \hat{n}_{-\frac{1}{2}} + \hat{n}_{-\frac{3}{2}} \hat{n}_{\frac{1}{2}} \right). \end{aligned}$$

Spin-spin correlations have been neglected here and there is no double-counting correction because we consider equivalent orbitals. Since Sr_2RhO_4 is paramagnetic at low temperature, we can set $\hat{n}_{\frac{3}{2}} = \hat{n}_{-\frac{3}{2}} \equiv \frac{1}{4}(\hat{n} - \hat{p})$ and $\hat{n}_{\frac{1}{2}} = \hat{n}_{-\frac{1}{2}} \equiv \frac{1}{4}(\hat{n} + \hat{p})$ with \hat{n} being the number of electrons in the two doubly-degenerate bands, and get:

$$\hat{H}_{\text{C}} \approx \frac{3U - 5J}{8} \hat{n}^2 - \frac{U - J}{8} \hat{p}^2 \approx c - \frac{U - J}{4} p \hat{p}.$$

The last expression is the mean-field approximation, which grouped together with \hat{H}_{SO} (4) yields a one-electron Hamiltonian with SO-coupled bands (2), but with ζ substituted by $\zeta_{\text{eff}} = \zeta + \frac{1}{2}(U - J)p$, and p determined self-consistently. The polarization function, $p(\zeta)$, may be found from the polarization of each Bloch state,

$$\left| c_{\pm; \frac{3}{2}}^{\mathbf{k}} \right|^2 - \left| c_{\pm; \frac{1}{2}}^{\mathbf{k}} \right|^2 = \frac{\partial \varepsilon_{\pm}^{\mathbf{k}}}{\partial \zeta / 2} = \frac{\pm \zeta}{\sqrt{(\varepsilon_{xz}^{\mathbf{k}} - \varepsilon_{yz}^{\mathbf{k}})^2 + \zeta^2}},$$

as follows from 1st-order perturbation theory. As a result:

$$p(\zeta) = 2\zeta \int_0^{\pi} \int_0^{\pi} \frac{dk_x dk_y}{\pi^2} \frac{\theta(\varepsilon_{+}^{\mathbf{k}}) \theta(-\varepsilon_{-}^{\mathbf{k}})}{\sqrt{(\varepsilon_{xz}^{\mathbf{k}} - \varepsilon_{yz}^{\mathbf{k}})^2 + \zeta^2}}.$$

where the factor 2 takes the double degeneracy of each band into account and we have used that $\theta(-\varepsilon_{-}^{\mathbf{k}}) - \theta(-\varepsilon_{+}^{\mathbf{k}}) = \theta(\varepsilon_{+}^{\mathbf{k}}) \theta(-\varepsilon_{-}^{\mathbf{k}})$. The integral is over the area between the $\bar{\Gamma}$ -centered electron sheet and the \bar{M} -centered hole sheet. For ζ large, $p(\zeta) \rightarrow 4 - n$, where n is the number of electrons in the xz and yz bands, and for ζ small, $p(\zeta) \rightarrow \chi_0 \zeta$ with the susceptibility

$$\chi_0 = 2 \int_0^{\pi} \int_0^{\pi} \frac{dk_x dk_y}{\pi^2} \frac{\theta(\varepsilon_{+}^{\mathbf{k}}) \theta(-\varepsilon_{-}^{\mathbf{k}})}{\varepsilon_{xz}^{\mathbf{k}} - \varepsilon_{yz}^{\mathbf{k}}} \approx \frac{1}{2(t_{\pi} - t_{\delta})}, \quad (5)$$

which turns out to be independent of n . The last approximation results from integrating over the rectangular $t_{\delta}=0$ area. The self-consistency condition, $\zeta_{\text{eff}} = \zeta + \frac{1}{2}(U - J)p(\zeta_{\text{eff}})$, thus yields a *Coulomb-enhanced SO coupling*, which for ζ_{eff} in the *linear* range of the polarization function is given by:

$$\frac{\zeta_{\text{eff}}}{\zeta} \approx \left[1 - \frac{U - J}{2} \chi_0 \right]^{-1} \approx \left[1 - \frac{U - J}{4(t_{\pi} - t_{\delta})} \right]^{-1}. \quad (6)$$

Inserting $\zeta_{\text{eff}}/\zeta = 2.15$ and $t_{\pi} - t_{\delta} = 0.146$ eV, we get: $U - J = 0.3$ eV and $p(\zeta_{\text{eff}}) = 0.97$, whereas using the proper polarization function, which saturates at

$p(\infty)=1$, yields: $U - J = 0.5\text{eV}$. This is a reasonable value for a $4d$ WO spreading onto the oxygen sites.

In order to substantiate this simple picture, we perform all-orbital relativistic LDA+U calculations [36] with U-J adjusted such as to give the best agreement with the ARPES FS. Since U and J in such calculations do not refer to proper orbitals, but to d-waves truncated and normalized inside atomic (LMTO) or muffin-tin (LAPW) spheres, the values of the parameters depend on the sphere size and are generally larger than for the more diffuse WOs [36]. As is obvious from Fig. 1 (LDA+U+SO), this agreement is even more perfect than for TB+'SO'; now even the small observed gaps [37] induced by the AF rotations are reproduced. The LDA+U+SO bands in Fig. 2 are well reproduced in the range from 0.15 eV below- to 0.5 eV above the Fermi level by the TB+'SO' bands folded into the BZ/2 with corners at \bar{X} . Features not reproduced are the tiny splittings due to in-plane xz - xy hopping and out-of-plane hoppings neglected in our TB model. The agreement between the TB and the LDA calculation is less satisfactory, first of all because without SO-quenching the in-plane xz - xy hopping produces a splitting along $\bar{\Gamma M}$, and secondly because the rotation-induced xy - $(x^2 - y^2)$ gapping is not complete without SO coupling. In fact, it takes the LDA+U+SO to push the lower edges of the xy - $(x^2 - y^2)$ gap to -0.16eV along $\bar{\Gamma M}$, and even deeper along $\bar{\Gamma X}$, locations close to those observed with ARPES [32]. Note finally, that the LDA+U alone, without SO coupling, brings little improvement compared with the LDA.

Having obtained perfect agreement with the ARPES FS, we use the LDA+U+SO to calculate cyclotron masses and compare with those obtained from the dHvA measurements [32]. The resulting enhancements are: $m_{\text{ARPES}}/m_{\text{LDA+U+SO}} = 2.1$ (α), 2.1 (β_M), and 2.3 (β_X). Consistently herewith the density of states at the Fermi level yields the electronic specific-heat enhancement: $\gamma_{\text{exp}}/\gamma_{\text{LDA+U+SO}} = 2.2$. These many-body enhancements are smaller than those (~ 3) in Sr_2RuO_4 .

We have finally performed relativistic LDA+U calculations also for Sr_2RuO_4 , and find the agreement with the experimental FS [28, 29, 30] to improve from good to perfect. Inclusion of SO+U in the LDA reduces the area of the α -pocket from 13 to 11% of the BZ-area in Sr_2RuO_4 , as compared with a 24 to 6% reduction in Sr_2RhO_4 . The stronger SO effects in the latter oxide are caused by ζ being 20% larger [39], due to the larger mass, and by the Coulomb enhancement (6) being larger due to the reduction of t_π caused by rotation. Other factors are similar in the two oxides because the extra hole in Sr_2RuO_4 is accommodated in the xy band, which hardly couples with the xz and yz bands. It is conceivable that reduction of t_π caused by Ca-induced rotations could make Coulomb-enhanced SO coupling of the xz and yz bands important in other ruthenates and rhodates not driven magnetic by the t -reduction.

In conclusion, resolution of the Sr_2RhO_4 puzzle has taught us that although usually neglected in $4d$ -oxides, the spin-orbit coupling belongs to the list of competing interactions which cause the rich physics of these materials [40].

-
- [1] A. Yamasaki *et al.*, Phys. Rev. Lett. **96**, 166401 (2006).
 - [2] A.I. Poteryaev *et al.*, Phys. Rev. B **76**, 085127 (2007).
 - [3] S. Y. Ezhov *et al.*, Phys. Rev. Lett. **83**, 4136 (1999).
 - [4] S. Nakatsuji *et al.*, Phys. Soc. Jpn **66**, 1868 (1997).
 - [5] M. Braden *et al.*, Phys. Rev. B **58**, 847 (1998).
 - [6] S. Nakatsuji *et al.*, Phys. Rev. Lett. **84**, 2666 (2000).
 - [7] O. Friedt *et al.*, Phys. Rev. B **63**, 174432 (2001);
 - [8] O. Friedt *et al.*, Phys. Rev. Lett. **93**, 147404 (2004).
 - [9] E. Pavarini *et al.*, New J. Phys. **7**, 188 (2005).
 - [10] K. Maiti, Phys. Rev. B **73**, 235110 (2006)
 - [11] I. Zegkinoglou *et al.*, Phys. Rev. Lett. **95**, 136401 (2005).
 - [12] K. T. Park, J. Phys. Condens. Matter **13**, 9231 (2001)
 - [13] Z. Fang *et al.*, Phys. Rev. B **69**, 045116 (2004)
 - [14] F. Nakamura *et al.*, Phys. Rev. B **65**, 220402(R) (2002).
 - [15] C.S. Snow *et al.*, Phys. Rev. Lett. **89**, 226401 (2002).
 - [16] P. Steffens *et al.*, Phys. Rev. B **72**, 094104 (2005).
 - [17] M. Kriener *et al.*, Phys. Rev. Lett. **95**, 267403 (2005).
 - [18] P. Steffens *et al.*, Phys. Rev. Lett. **99**, 217402 (2007).
 - [19] T. Oguchi, Phys. Rev. B **51**, 1385(R) (1995).
 - [20] D. J. Singh, Phys. Rev. B **52**, 1358 (1995).
 - [21] L. M. Woods, Phys. Rev. B **62**, 7833 (2000)
 - [22] Z. Fang *et al.*, Phys. Rev. B **64**, 020509(R) (2001)
 - [23] K. Maiti *et al.*, Phys. Rev. B **71**, 161102(R) (2005)
 - [24] D.J. Singh *et al.*, Phys. Rev. Lett. **96**, 097203 (2006)
 - [25] S.-C. Wang *et al.*, Phys. Rev. Lett. **93**, 177007 (2004).
 - [26] Y. Maeno *et al.*, Nature (London) **372**, 532 (1994).
 - [27] A.P. Mackenzie *et al.*, Rev. Mod. Phys. **75**, 657 (2003)
 - [28] A.P. Mackenzie *et al.*, Phys. Rev. Lett. **76**, 3786 (1996).
 - [29] A. Damascelli *et al.*, Phys. Rev. Lett. **85**, 5194 (2000).
 - [30] N.J.C. Ingle *et al.*, Phys. Rev. B **72**, 205114 (2005)
 - [31] B. J. Kim *et al.*, Phys. Rev. Lett. **97**, 106401 (2006).
 - [32] R.S. Perry *et al.*, New J. Phys. **8**, 175 (2006).
 - [33] F. Baumberger *et al.*, Phys. Rev. Lett. **96**, 246402 (2006).
 - [34] E. Ko *et al.*, Phys. Rev. Lett. **98**, 226401 (2007).
 - [35] T. Vogt and D. J. Buttrey, J. Solid State Chem. **123**, 186 (1996); $T=4\text{K}$, space group: $I4_1/acd$. Compared with the bct K_2NiF_4 -type structure, the cell is doubled in the plane due to the alternating rotations of neighboring RhO_6 octaheda, and also in the z -direction due to alternating rotations in every 3rd RhO_2 plane.
 - [36] The calculations were performed for the correct structure [35] using RLAPW software for accuracy (K. Schwarz *et al.*, Comput. Phys. Commun. **147**, 71 (2002)) and RLMTTO software for speed and interpretation (V. N. Antonov *et al.*, J. Magn. Magn. Mater. **146**, 205 (1995)). The space filling spheres of the latter method were chosen such that the bands were identical with those from the former. The LDA results shown in the figures agree with those previously published [31, 33]. The LDA+U(+SO) (R)LMTO calculations used $U=2.5\text{eV}$ and $J=0.9\text{eV}$ for the Rh d partial waves in the Rh sphere.
 - [37] FIG. 3 in [33], TABLE I in [38] and p. 17 in [9].
 - [38] E. Pavarini and I.I. Mazin, Phys. Rev. B **74**, 035115 (2006); *ibid* **76**, 079901(E) (2007). The 500 K scale in

Fig. 2 is several times too big.

- [39] A.R. Mackintosh and O.K. Andersen in *Electrons at the Fermi Surface*, ed. M. Springford, CUP, Cambridge 1980.
- [40] Important SO effects in Ca-ruthenates were anticipated

by T. Mizokawa *et al.*, Phys. Rev. Lett. **87**, 077202 (2001)
and Z. Fang *et al.*, New J. Phys. **7**, 66 (2005).